



Original Research Article

Mir-155-5p targets TP53INP1 to promote proliferative phenotype in hypersensitivity pneumonitis lung fibroblasts

Marco Espina-Ordoñez^{a,b}, Yalbi Itzel Balderas-Martínez^c, Ana Lilia Torres-Machorro^d,
Iliana Herrera^a, Mariel Maldonado^a, Yair Romero^e, Fernanda Toscano-Marquez^a,
Annie Pardo^e, Moisés Selman^a, José Cisneros^{f,*}

^a Laboratorio de Biopatología Pulmonar INER-Ciencias-UNAM, Instituto Nacional de Enfermedades Respiratorias Ismael Cosío Villegas, Ciudad de México, 14080, Mexico

^b Posgrado en Ciencias Biológicas, Unidad de Posgrado, Edificio D, Piso 1, Circuito de Posgrados, Ciudad Universidad, Coyoacán, C.P 04510, CDMX, Mexico

^c Laboratorio de Biología Computacional, Instituto Nacional de Enfermedades Respiratorias Ismael Cosío Villegas, Ciudad de México, 14080, Mexico

^d Laboratorio de Biología Celular, Instituto Nacional de Enfermedades Respiratorias Ismael Cosío Villegas, Ciudad de México, 14080, Mexico

^e Facultad de Ciencias, Universidad Nacional Autónoma de México, Ciudad de México, 04510, Mexico

^f Departamento de Investigación en Fibrosis Pulmonar, Instituto Nacional de Enfermedades Respiratorias Ismael Cosío Villegas, Ciudad de México, 14080, Mexico



ARTICLE INFO

Keywords:
Pneumonitis
Computational biology
MicroRNAs
Lung
Fibroblasts

ABSTRACT

Background: Hypersensitivity pneumonitis (HP) is an inflammatory disorder affecting lung parenchyma and often evolves into fibrosis (fHP). The altered regulation of genes involved in the pathogenesis of the disease is not well comprehended, while the role of microRNAs in lung fibroblasts remains unexplored.

Methods: We used integrated bulk RNA-Seq and enrichment pathway bioinformatic analyses to identify differentially expressed (DE)-miRNAs and genes (DEGs) associated with HP lungs. In vitro, we evaluated the expression and potential role of miR-155-5p in the phenotype of fHP lung fibroblasts. Loss and gain assays were used to demonstrate the impact of miR-155-5p on fibroblast functions. In addition, miR-155-5p and its target TP53INP1 were analyzed after treatment with TGF- β , IL-4, and IL-17A.

Results: We found around 50 DEGs shared by several databases that differentiate HP from control and IPF lungs, constituting a unique HP lung transcriptional signature. Additionally, we reveal 18 DE-miRNAs that may regulate these DEGs. Among the candidates likely associated with HP pathogenesis was miR-155-5p. Our findings indicate that increased miR-155-5p in fHP fibroblasts coincides with reduced TP53INP1 expression, high proliferative capacity, and a lack of senescence markers compared to IPF fibroblasts. Induced overexpression of miR-155-5p in normal fibroblasts remarkably increases the proliferation rate and decreases TP53INP1 expression. Conversely, miR-155-5p inhibition reduces proliferation and increases senescence markers. TGF- β , IL-4, and IL-17A stimulated miR-155-5p overexpression in HP lung fibroblasts.

Conclusion: Our findings suggest a distinctive signature of 53 DEGs in HP, including CLDN18, EEF2, CXCL9, PLA2G2D, and ZNF683, as potential targets for future studies. Likewise, 18 miRNAs, including miR-155-5p, could be helpful to establish differences between these two pathologies. The overexpression of miR-155-5p and downregulation of TP53INP1 in fHP lung fibroblasts may be involved in his proliferative and profibrotic phenotype. These findings may help differentiate and characterize their pathogenic features and understand their role in the disease.

1. Introduction

Hypersensitivity pneumonitis (HP) is a lung disorder with varying degrees of inflammation and fibrosis affecting lung parenchyma. The disease is classified as non-fibrotic and fibrotic (a mixture of

inflammation and fibrosis) [1,2]. HP is the second most common interstitial lung disease (ILD), with features of progressive fibrosis in up to 81% of cases, and most cases of fibrotic HP (fHP) result from antigens inhalation from feathers and bird droppings [3]. The fibrotic form of HP is the main mimicker of idiopathic pulmonary fibrosis (IPF), especially if

* Corresponding author.

E-mail address: jcisneros828@gmail.com (J. Cisneros).

<https://doi.org/10.1016/j.ncrna.2024.02.010>

Received 19 October 2023; Received in revised form 11 February 2024; Accepted 19 February 2024

Available online 11 March 2024

2468-0540/© 2024 The Authors. Publishing services by Elsevier B.V. on behalf of KeAi Communications Co. Ltd. This is an open access article under the CC BY-NC-ND license (<http://creativecommons.org/licenses/by-nc-nd/4.0/>).

it shows the usual interstitial pneumonia (UIP) pattern [4], making it difficult to diagnose. Although there is progress in the study of the pathogenesis of HP, the molecular mechanisms governing the phenotype of the cells involved in its development and progression remain poorly understood, and they could help distinguish it from IPF [5,6].

MicroRNAs (miRNAs) participate in several pathological processes, including fibrosis in tissues like the kidney, liver, and lung [7]. To date, 2654 miRNAs are annotated in the miRBase database version 22 and regulate more than 60% of the human transcripts [8]. There is evidence that specific miRNAs are involved in the phenotype of IPF fibroblasts [9, 10]; however, no study has investigated the role of miRNAs in HP.

The miR-155-5p is involved in the pathogenesis of several diseases as its aberrant expression is associated with cellular mechanisms such as inflammation, proliferation, apoptosis, and fibrosis [11–15]. In lung fibroblasts, miRNA-155 expression increases by inflammatory stimuli such as interleukin-1 β (IL-1 β) and tumor necrosis factor- α (TNF- α), while it is decreased by transforming growth factor β (TGF- β) [16]. Additionally, it has been suggested that miR-155-5p is a critical regulatory microRNA in IPF pathogenesis [17].

This study aimed to identify differentially expressed miRNAs and genes by integrating the available HP bulk RNA-Seq data to determine the biological processes possibly implicated in the pathogenesis and to investigate the putative role of miR-155-5p in the fibroblast phenotype.

2. Materials and methods

2.1. Antibodies and reagents

Advanced DMEM/F12 1x (Life Technologies, Thermo Fisher Scientific, Hudson, NH), Fetal Bovine Serum (Thermo Fisher Scientific, Hudson, NH, 23235), 0.25% Trypsin-EDTA 1x (Thermo Fisher Scientific, Hudson, NH, 23235), 1x antimicrobial agent Primocin (InvivoGen, San Diego, CA), recombinant human TGF- β 1 (Biolegend, San Diego, CA), recombinant human IL-17A (Biolegend, San Diego, CA), recombinant human IL-4 (Biolegend, San Diego, CA), Cellular Senescence Assay kit (Merck, Darmstadt, Germany), microRNA Purification Kit (Norgen Biotek Corp, ON, Canada), taqMan Advanced miRNA cDNA Synthesis Kit (Thermo Fisher Scientific, Hudson, NH), TaqMan Advanced miRNA Assays, verso cDNA synthesis kit (Thermo Fisher Scientific, Hudson, NH), CyQuant NF Cell proliferation assay kit (Invitrogen, Grand Island, NY), Precision plus protein dual color standard (Bio-Rad Laboratories, Hercules, CA), antibody diluent reagent solution ready-to-use (Invitrogen, Grand Island, NY), Pierce RIPA Buffer (Thermo Fisher Scientific, Hudson, NH), protease inhibitor cocktail 100x (Bioss, Woburn, MA), Halt phosphatase inhibitor cocktail 100x (Thermo Fisher Scientific, Hudson, NH), nitrocellulose membrane 0.45 μ m (Bio-Rad Laboratories, Hercules, CA), Micro BCA protein assay kit (Thermo Fisher Scientific, Hudson, NH, 23235), 4x laemli sample buffer (Bio-Rad Laboratories, Hercules, CA), Intercept Blocking Buffer (LI-COR Biosciences, Lincoln, NE), human anti-p21 (Santa Cruz, Biotechnology, Santa Cruz, CA), human anti-p53 (R&D), human anti-TP53INP1 (Abcam, Cambridge, MA), human anti-GAPDH (Cloud Clone), 4',6-diamidino-2-phenylindole (DAPI), Odyssey[®] CLx Molecular Imaging Workstation, fluorescent secondary antibodies IRDye 680RD and IRDye800CW (LI-COR Biosciences, Lincoln, NE), premade adenoviral system Null condition and for miR-155-5 ON and OFF (Applied Biological Materials Inc, Richmond, BC, Canada), hydrophilic polycarbonate membrane with 8 μ m diameter filters (Millipore Corp, Burlington, MA) and precoated with 50 μ l of purified collagen type I (4.07 mg/ml, Corning), 48-well plate with a circular insert of approximately 1 mm diameter made of polydimethylsiloxane (PDMS), a microplate reader Synergy Biotek H1 (Agilent Technologies, Santa Clara, CA), biotinylated secondary antibody (Biogenex, San Ramón, CA, USA) and 3-Amino-9-ethyl carbazole (AEC) (Biogenex, San Ramón, CA, USA) chromogen.

2.2. Ethics statement and experimental design

The Ethic, Scientific, and Biosecurity Committees of the Instituto Nacional de Enfermedades Respiratorias Ismael Cosío Villegas approved the research under protocol number B09-13. We used lung fibroblasts from the cell Biobank of our laboratory. Cells were obtained from lung biopsies for diagnosis in patients who signed written informed consent. Normal human lung fibroblasts (controls) were obtained from donors without lung disease who died from an accident (n = 3). Normal lung fibroblasts from Lonza (NHLF cell line, Walkersville, Inc.) were also used. The identification and personal data of all participants were kept anonymous and protected.

2.3. Selection of high-throughput studies

We used the microarray and RNA-seq raw data from HP-related miRNA and mRNA expression profiles from the National Center for Biotechnology Information (NCBI)-Gene Expression Omnibus (GEO) database (<https://www.ncbi.nlm.nih.gov/geo/>) tapping "Hypersensitivity Pneumonitis" as a keyword. We downloaded the miRNA expression microarray dataset GSE21394 and the mRNA GSE21369, both contained in the superseries GSE21411 [18] and the mRNA expression RNA-seq dataset GSE150910 [19]. We could not obtain raw data from one study [20] but used the results reported in the original article. These data were manually curated using NCBI databases to update gene names and remove duplicate and non-coding elements (opposite strands and introns of known genes). Only data from HP, IPF, and control tissue lung samples were analyzed according to Fig. S1.

2.4. Analysis of differential expression in genes and miRNAs

We used R software version 4.1.0 and Bioconductor v.3.13 [21] for analyzing RNA microarray and RNA-seq data, which were pre-processed and normalized following general pipelines from Limma v3.48.3 [22] and DESeq2 v1.32.0 [23] packages, respectively. Genes were considered differentially expressed among HP, control, and IPF lung samples if they had an adjusted p-value <0.05 and a |log fold change (FC)| > 1.0 as cut-off criteria (except for HP vs. IPF from GSE21369, where we used p-value <0.005 and a |log FC| > 1.0). We used a p-value <0.001 and a |log FC| > 0.5 for the miRNA array as cut-off criteria. Additionally, with a Venn diagram, we analyze the DEGs associated with both pathologies and the pathways that enrich them, as described below.

2.5. Pathway enrichment analysis

We performed an enrichment pathway analysis with consistent differentially expressed genes (DEGs) in at least two expression profile datasets using the EnrichR package v3.0 (<https://CRAN.R-project.org/package=enrichR>) [24] and MsigDB Hallmark 2020 database [25]. Pathways with a significant enrichment have an adjusted p-value <0.05. We used the ggplot2 package v.3.3.6 (<https://ggplot2.tidyverse.org>) [26] to generate the graphs to visualize the pathway enrichment analysis.

2.6. Identification of miRNAs with validated interactions with DEGs

As an alternative to identify miRNAs with potential roles in HP pathogenesis, we used the DEGs of each experiment for each contrast (HP vs. Ctrl, HP vs. IPF, and IPF vs. Ctrl) to identify the miRNAs that have validated interactions with them. This identification was made online with the web tool MIENTURNET (<http://userver.bio.uniroma1.it/apps/mienturnet/>) (02-23-2022) [27]. We used the database miRTarBase 7.0 [28], which only considered experimentally validated miRNA-target interactions, to select the miRNAs with at least 20 interactions with DEGs of each contrast. The intersection between the identified miRNAs for HP vs. Ctrl and HP vs. IPF were considered

miRNAs that could have potential roles in the pathogenesis of HP. From the list obtained and with a literature search of miRNAs associated with fibrosis, we selected miR-155-5, a microRNA associated with multiple processes involved in its pathogenesis [15], recently proposed as a critical orchestrator in IPF [17] and unknown in the HP field, particularly in isolated fibroblasts. We built an interaction network to summarize the DEGs between HP lungs compared to IPF lungs that were validated targets of this microRNA using Cytoscape version 3.8.0 [29].

2.7. Cell culture and treatments

We used fibroblasts derived from lung tissue of fibrotic HP (n = 4), age 54 ± 6.27 years 2F (female)/2 M (male), and IPF (n = 4), age 63 ± 6.37 years 1F/3 M patients. Diagnosing HP and IPF was performed as described and confirmed by histopathology [20]. HP patients were positive for avian antigens as an inducer of the disease. Control fibroblasts (n = 4), age 61.75 ± 9.39 years, 2F/2 M, were obtained from the lungs of cadaveric donors without lung disease (n = 3), and one acquired from Lonza (NHLF cell line, Walkersville, Inc.).

Fibroblasts in passage five were cultured in Advanced DMEM/F12 (Thermo Fisher Scientific) supplemented with 5% fetal bovine serum (FBS), 1x L-glutamine, and 1x antimicrobial agent Primocin (Invivogen) at 37 °C in an atmosphere of 5% CO₂ and 95% air humidity. At 80% confluence, the cells were routinely passaged by trypsinization. Cells were fixed for senescence assay or lysed to obtain cell extracts for Western blotting or mRNA and miRNA extraction. TGF-β, IL-17A, and IL-4 (Biolegend) were used at 10 ng/ml for 24 h.

2.8. Senescence-associated β-galactosidase assay

β-galactosidase activity was performed in basal conditions or 72h post-transduction with miR-155 adenoviral particles using the Cellular Senescence Assay kit (Merck, Darmstadt, Germany) following the manufacturer's instructions. Images were acquired in an Olympus IX81 inverted microscope and then manually quantified using Fiji V1.53 software [30]. The β galactosidase positive cells were determined over ten random fields from two replicates.

2.9. miRNA and mRNA expression analysis

The miRNAs and mRNA were obtained with a microRNA Purification Kit (Norgen Biotek Corp, ON, Canada) and reverse transcribed with TaqMan Advanced miRNA cDNA Synthesis Kit (Thermo Scientific, Waltham, MA, USA) following the manufacturer's instructions. The miR-155-5p expression was measured by real-time PCR using the TaqMan Advanced miRNA Assays, and miR-191-5p was used as a normalizer as determined by Bestkeeper V1 software [31] in our conditions (power of HKG: 1.62, SD: 0.79). To mRNA, cDNA was synthesized with verso cDNA synthesis kit (Thermo Scientific) to evaluate the expression of COL1A1, COL3A1, p21, p53, TP53INP1, PCNA, Ki-67, and HPRT using specific primers (Table S1). The relative expression of targets was calculated using $2^{-\Delta\Delta Ct}$ of the triplicates of three independent experiments.

2.10. Western blot analysis

Cells were lysed in RIPA buffer (Sigma-Aldrich Corporation) containing protease and phosphatase inhibitors. Protein concentration was measured with the micro BCA assay protein assay kit (Thermo Scientific). The proteins (25 μg) were separated by SDS-PAGE and transferred into nitrocellulose membranes (Bio-Rad Laboratories Inc), blocked with Intercept Blocking Buffer (LI-COR Biosciences), and incubated overnight at 4 °C with primary antibodies against p21 (Santa Cruz sc-6246; 1:500), p53 (R&D AF1355; 1:1000), TP53INP1 (Abcam ab202026; 1:2000), and GAPDH (Cloud Clone PAB932Hu01; 1:4000). After washing with TBS-Tween 0.05%, the fluorescent signal was detected and captured in an

Odyssey® CLx Molecular Imaging Workstation using fluorescent secondary antibodies IRDye 680RD and IRDye800CW (LI-COR Biosciences). The intensity of target proteins relative to GAPDH was calculated with Fiji V1.53 software.

2.11. Immunocytochemistry (ICC)

Fibroblasts were grown on coverslips, fixed with paraformaldehyde 4% for 20 min, treated for 20 min with Universal Blocking Reagent (Biogenex, San Ramon, CA, USA), and then incubated with a rabbit anti-human TP53INP1 (ab202026, Abcam, Cambridge, UK; 1:250 dilution) overnight at 4 °C. The cells were incubated with a secondary antibody (donkey anti-rabbit DyLight-488; 1:450 dilution) for 1 h at room temperature incubated with DAPI for 10 min at room temperature, and then rinsed twice with PBS and mounted with Mowiol medium. Images were obtained with a microscope (Olympus, FsV1000) using a UPlan-FLN 40 NA 1.3 objective. Images were processed using Fiji V1.53 software.

2.12. Immunohistochemistry (IHC)

Immunohistochemical analysis was performed on lung tissues from patients with HP and IPF. Endogenous peroxidase was blocked, and antigen recovery was performed using citrate buffer at pH 6. Tissues were incubated with Universal Blocking Solution 1x (Biogenex, San Ramon, CA, USA) for 30 min and then with the TP53INP1 primary antibody (ab202026, Abcam, Cambridge, UK; 1:150 dilution) at 4 °C overnight. After treatment with a biotinylated secondary antibody and streptavidin coupled with a horseradish peroxidase-conjugated secondary antibody system from Biogenex (San Ramon, CA, USA), the immunodetection was performed using acetate buffer containing 0.05% H₂O₂ and 3-Amino-9-ethyl carbazole. The tissues were counterstained with hematoxylin, and nonimmune serum was used as a negative control. Images were captured using a Leica DM3000.

2.13. Adenoviral transduction of lung fibroblasts

Adenoviral transduction of miR-155-5p on fibroblasts with a pre-made adenoviral system (Applied Biological Materials Inc) was done following the manufacturer's instructions. All experiments where we used transduced fibroblasts started 24h after the transduction with adenoviral particles (MOI 100) from null construction (Null), pre-miR-155-5p sequence (miR-155 ON), or the inhibitory sequence for miR-155-5p (miR-155 OFF).

2.14. Proliferation assay

Lung fibroblasts were seeded in 96-well plates (5000 cells/well) and attached for 12 h. After transduction, the proliferating cells were determined at basal, 24, 48, and 72 h using the CyQuant NF Cell Proliferation Assay (Life Technologies). CyQuant NF dye reagent diluted in 1x Hank's balanced salt solution (HBSS) buffer (50 μL) was added to the cells and incubated at 37 °C for 30 min. Fluorescence values were acquired in a microplate reader (Synergy Biotek H1, Agilent) with a 485/530 nm excitation/emission filter. Experiments were performed in triplicate.

2.15. Migration assays

Migration assays were performed using a transwell 96-well plate with a hydrophilic polycarbonate membrane with 8 μm diameter filters (Millipore Corporation) and precoated with 50 μl of purified collagen type I (4.07 mg/ml, Corning). Fibroblasts (5×10^5) were seeded in serum-free DMEM/F12 in the upper chamber, and DMEM/F12 media supplemented with 5% FBS was added to the lower chamber. After 18 h, cells that migrated through the membrane were fixed in 1% glutaraldehyde for 20 min and stained with 0.1% crystal violet. The dye was

recovered in 200 µl of 10% acetic acid solution, and absorbance values were determined at 590 nm. The experiments were performed twice in duplicate.

In addition, migration was evaluated using a wound-healing assay. Briefly, transduced fibroblasts (2 × 105) were seeded in a 48-well plate with a circular insert of approximately 1 mm diameter made of polydimethylsiloxane (PDMS). After 12 h, the insert was removed, the medium was replaced with fresh medium, and photographs of wound closure were taken under an inverted microscope at 0, 24, and 48 h. Experiments were performed in duplicate, and the percentage of wound expansion was calculated using Fiji V1.53 software.

2.16. Statistical analysis

Graphical presentation of data and statistical analysis were performed using GraphPad Prism v.8.0.1 [32]. All data are expressed as mean ± standard deviation and were analyzed using one-way or two-way ANOVA with Tukey’s multiple comparison test. Differences between groups were considered significant at a p-value <0.05.

3. Results

3.1. Integrated analysis of datasets identified common DEGs in HP lungs

We found four datasets related to HP performed in lung tissue samples for the bulk RNA-Seq analysis, and no data were available for HP lung fibroblasts. Three of the four come from mRNA expression profiles. The first dataset from Selman et al. includes data from 12 HP and 15 IPF samples from which we could not obtain the raw data, and the genes were manually updated [20]. The second profile was generated by the array expression deposited in the GSE21369 [18], and we used 5 controls, 2 HP, and 7 IPF samples that approved the quality analysis. The third dataset, GSE150910, was generated from RNA-seq data of 103 controls, 86 chronic HP, and 103 IPF lung tissue samples [19]. Finally, an HP-related miRNA array was found, deposited as the GSE21394 [18], and containing data from 6 control samples, 2 HP samples, and 9 IPF samples (Table 1).

Using a bioinformatics pipeline with R Bioconductor, we determined the DEGs of each experiment. In the study by Selman et al., they identified 809 DEGs between HP and IPF lung samples (301 upregulated genes in IPF lung and 508 upregulated genes in HP lungs) (Table S2). For GSE21369, 317 DEGs for HP vs. Ctrl, 118 for HP vs. IPF, and 261 for IPF vs. Ctrl (Table S3). For GSE150910, 2198 DEGs for HP vs. Ctrl, 569 for HP vs. IPF, and 1928 for IPF vs. Ctrl (Table S4). Furthermore, common DEGs with the same expression trend in at least two profile datasets were identified (Table S5): 46 between HP and control lungs, 53 in the HP vs. IPF contrast, and 53 between IPF and control lungs. Using a Venn diagram, we find that 10 DEGs are shared between HP and IPF (Fig. S2).

Table 1

miRNA and gene expression microarray and RNA-seq datasets related to Hypersensitivity Pneumonitis. *Samples of other ILDs that were not HP and IPF were excluded. +Samples that did not approve the quality analysis were excluded.

RNA type	Accession number of the dataset	Platform	Sample type	Experiment type	Disease type			Number of differentially expressed genes	Reference
					Ctrl	HP	IPF		
miRNA	GSE21394	Agilent-019118 Human miRNA Microarray 2.0 G4470B	Lung tissue	Non-coding RNA profiling by array	6	2	9	HP vs CTRL = 23 HP vs IPF = 31 IPF vs CTRL = 65	Cho J et al., <i>BioMed Central</i> , 2011*
mRNA	GSE21369	Affymetrix U133 plus 2.0 Array	Lung tissue	Expression profiling by array	5	2	7	HP vs CTRL = 317 HP vs IPF = 118 IPF vs CTRL = 261	Cho J et al., <i>BioMed Central</i> , 2011*+
mRNA	-	Affymetrix U133 plus 2.0 Array	Lung tissue	Expression profiling by array	-	12	15	HP vs IPF = 809	Selman M et al., <i>Am J Respir Crit Care Med</i> , 2006
mRNA	GSE150910	Illumina NovaSeq 6000 (Homo sapiens)	Lung tissue	Expression profiling by RNA-seq	103	82	103	HP vs CTRL = 2198 HP vs IPF = 569 IPF vs CTRL = 1928	Furusawa H et al. <i>Am J Respir Crit Care Med</i> , 2020

Table 2

Common differently expressed genes in each comparison. The common top ten most upregulated and downregulated genes were identified from three cohort profile data sets in each comparison. The logFC was retrieved from GSE21369 or GSE150910*, depending on the case.

Common DEGs in HP vs. Ctrl	logFC	Common DEGs in HP vs. IPF	logFC	Common DEGs in IPF vs. CTRL	logFC
CARMN	3.93	CLDN18*	3.32	FNDC1	2.89
DIO2	3.77	EEF2*	3.25	COL3A1	2.73
FNDC1	3.58	CXCL9*	2.6	CARMN	2.44
FAM83D	3.36	PLA2G2D*	2.42	DIO2	2.42
COL15A1	3.3	ZNF683*	2.147	VSIG1	2.3
COL3A1	3.22	LMOD1*	2.09	FLNC	2.28
DES	3.08	SPRR1A	2.07	DDX17	1.9
FBX032	2.59	SORBS1	2	THY1	1.89
LMOD1	2.56	COL4A6	1.9	COL1A2	1.87
FLNC	2.28	AGER*	1.8	PWWP3A	1.87
RGCC	-1.78	CLMP*	-1.08	SLC19A3	-1.79
KLF6	-1.83	CCL24*	-1.09	MME	-1.84
RAB11FIP1	-1.94	SEMA3C*	-1.17	AGTR2	-1.94
PAPSS2	-1.96	BHMT2*	-1.175	GADD45B	-2.04
SLC19A3	-2.01	F11R*	-1.24	HHIP	-2.04
EPB41L5	-2.48	JAG1*	-1.25	PIGA	-2.08
MYRF	-2.66	MAP1B*	-1.34	GPM6A	-2.11
SLC39A8	-2.71	IRF4*	-1.599	KLF4	-2.24
FAM167A	-2.93	CLIC5	-1.65	NAMPT	-2.29
CA4	-4.4	LAMP3*	-2.03	IL1RL1	-3.86

Table 2 lists the top ten up-and down-regulated genes in each contrast, with CLDN18, EEF2, CXCL9, PLA2G2D, and ZNF683 standing out as the most over-expressed genes between HP and IPF.

Moreover, we identified 23 DE-miRNAs in HP vs. Ctrl, 31 in HP vs. IPF, and 65 in IPF vs. Ctrl in the GSE21394, which contains the unique miRNA microarray available for HP (Table S6).

3.2. Common DEGs enriched pathways such as EMT, inflammatory, and immune response in HP lungs

To identify the possible pathways in which the DGEs are involved, a functional analysis was performed using EnrichR and the Kyoto Encyclopedia of Genes and Genomes (KEGG), Molecular Signatures Database (MSigDB), and Gene Ontology Biological Process (GOBP) databases. MsigDB is a collection that summarizes and represents specific and well-defined biological states or processes and displays coherent expression [25]. Fig. 1 illustrates the enriched pathways according to the MSigDB database. The functional analysis revealed that DEGs between HP and control lungs are significantly associated with the epithelial-mesenchymal transition (EMT), myogenesis, angiogenesis, UV response, and apical junction. Moreover, pathways related to graft rejection, interferon α/γ response, myogenesis, EMT, and inflammatory

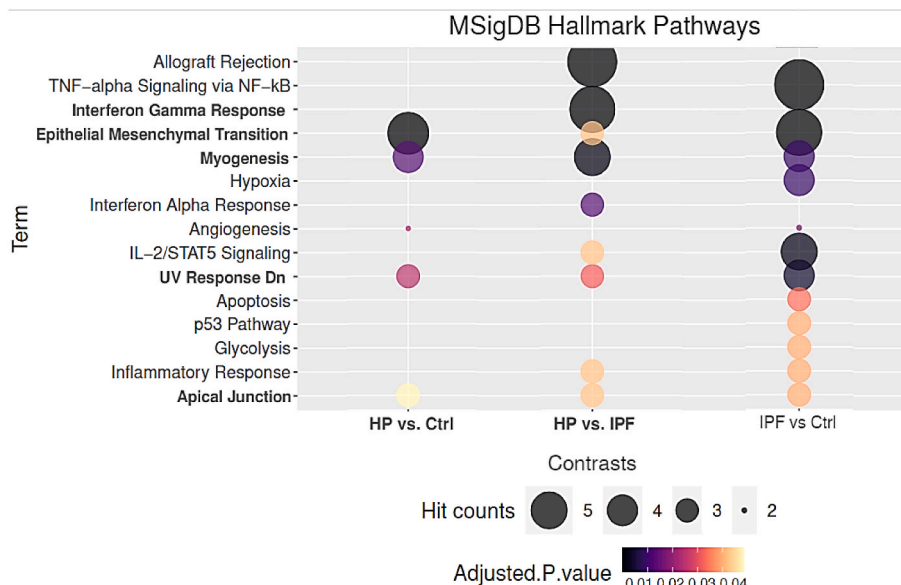


Fig. 1. Enriched MSigDB pathways obtained from DEGs in HP lungs. The MSigDB enriched pathways (adjusted p-value <0.05) using the common DEGs in each contrast. Colors indicate adjusted p-values, and circle size indicates the number of identified genes in each pathway.

response were enriched in DEGs between HP and IPF lungs. Finally, TNF- α /signaling nuclear factor-kappa B (NF-kB), EMT, hypoxia, apoptosis, and p53 pathway were enriched terms for the DEGs in IPF vs. Ctrl contrast. The enhanced ways for each comparison according to KEGG and GOBP databases are shown in Tables S7 and S8, respectively. These results showed that most DEGs enriched pathways related to mechanisms involved in pulmonary fibrosis, such as EMT and apical junction. However, common pathways such as myogenesis and angiogenesis were also enriched among the three contrasts, suggesting that these mechanisms are involved to different degrees in both pathologies. In addition, pathways such as inflammatory response, allograft rejection, and interferon-gamma (IFN- γ) response are involved in the pathogenesis of HP. Similar results were found when DEGs were analyzed using a Venn diagram, and in addition, IL-2/STAT5 signaling, myogenesis, and angiogenesis were the pathways enriched from the intersection between HP and IPF (Fig. S2).

3.3. miRNA enrichment analysis identified miR-155-5p as a candidate miRNA associated with HP pathogenesis

Using mirTarBase, we determined the miRNAs with experimental

evidence supporting a role in the regulation of DEGs in each dataset for each comparison (Table S9) and the common miRNA in at least two data sets between HP vs. Ctrl and HP vs. IPF (Table S10). Fig. 2A enlists the 18 miRNAs that resulted from the overlap between the identified miRNAs for HP vs. Ctrl and HP vs. IPF contrasts. We consider them candidate miRNAs associated with HP pathogenesis because they can regulate DEGs in HP compared to control and IPF lungs. We were interested in experimentally evaluate hsa-miR-155-5p in HP lung fibroblasts because it is a multifunctional miRNA extensively studied in various diseases, including fibrotic and inflammatory disorders [15,33], and it has been suggested as a critical miRNA involved in the pathogenesis of IPF [17]. miR-155 participates in mechanisms that affect proliferation and senescence, two processes involved in different pathways associated with fibrosis development and progression, including EMT, inflammation, and myogenesis; however, its role in HP lung fibroblasts remains unknown.

3.4. miR-155-5p is upregulated in fHP lung fibroblasts

MiR-155-5p is involved in critical processes implied in fibrosis. Therefore, we initially assessed the basal levels of miR-155-5p

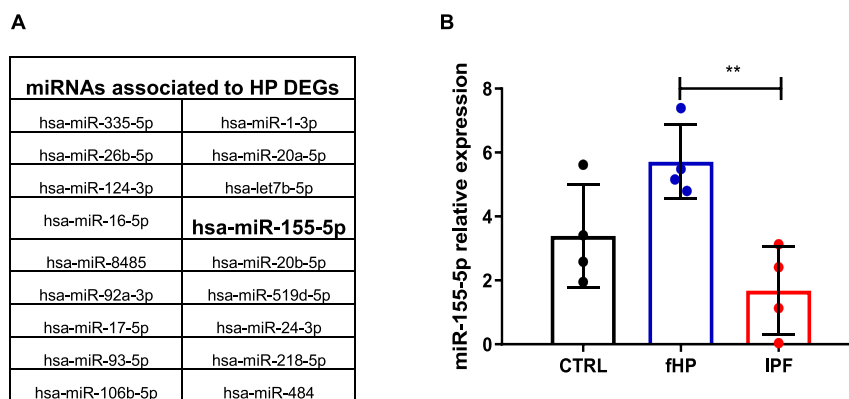


Fig. 2. miRNAs enrichment analysis identified miR-155-5p and is overexpressed in fHP lung fibroblasts. (A) Top candidate miRNAs with validated interactions with the DEGs in HP lungs compared to control and IPF. The miRNAs are listed in descending order from top to bottom according to the number of interactions. (B) Basal expression of miR-155-5p determined by qPCR (n = 4 per group). Data are presented as mean \pm SD by one-way ANOVA. The results represent three independent experiments**p < 0.01. CTRL: controls; fHP: hypersensitivity pneumonitis; IPF: idiopathic pulmonary fibrosis.

expression in control, fHP, and IPF lung fibroblast cultures. Remarkably, we found a three-fold increase of miR-155-5p in fHP lung fibroblasts compared with IPF fibroblasts ($p < 0.01$ Fig. 2B). This differential expression suggests that miR-155-5p may play a role in the behavior of HP fibroblasts and regulate some differences concerning control and IPF.

3.5. HP lung fibroblasts do not express senescence markers

Several microRNAs have been linked to the senescence process, and miR-155-5p is negatively regulated by p53. Since we found an increase of miR-155-5p in fHP fibroblasts and p53 belongs to a pathway that regulates the establishment of cellular senescence [34], we examined senescence markers in fibroblasts growing under basal conditions. As demonstrated in Fig. 3, fHP and control fibroblasts did not exhibit β -galactosidase positive cells compared to age and passage-matched IPF fibroblasts, where a significant increase in this marker was observed (Fig. 3A and B). Additionally, there was a substantial increase of p53 (Fig. 3C) and p21 (Fig. 3D) in IPF fibroblasts compared to fHP and control. Consistently, protein expression of p53 and p21 was significantly increased in IPF fibroblasts compared to HP, while no differences in p21 and p53 levels between HP and control fibroblasts were observed (Fig. 3E). These results suggest that the senescence is not part of the phenotype of fHP fibroblasts and that the upregulation of miR-155-5p may contribute to this observation.

3.6. HP lung fibroblasts are characterized by proliferative phenotype

MiR-155-5p induces cell proliferation, including fibroblasts [35]. Consequently, we examined the proliferative capacity of fHP fibroblasts, which overexpress miR-155-5p. As shown in Fig. 4A, fHP fibroblasts exhibit a heightened proliferative capacity compared to control and IPF fibroblasts. In addition, these cells also showed increased expression of the proliferation-associated genes ki-67 and PCNA (Fig. 4B and C). These results indicate that fHP fibroblasts have a distinctive phenotype characterized by an increased capacity for proliferation.

3.7. TP53INP1 is decreased in fHP lung fibroblasts

To investigate the potential link between increased proliferation and miR-155-5p expression and identify validated targets associated with this phenotype, we analyzed the miR-155-5p interaction network with DEGs between fHP and IPF fibroblasts (Fig. 5A). Among these, we identified as one of the most downregulated genes, the Tumor Protein P53 Inducible Nuclear Protein 1 (TP53INP1), which is an anti-proliferative protein overexpressed in IPF lungs [20] and a conserved target of miR-155-5p (Fig. 5B). Interestingly, analysis of TP53INP1 by qPCR and immunoblot shows a significant reduction of TP53INP1 at the gene and protein levels in fHP fibroblasts compared with IPF fibroblasts (Fig. 5C–E and Fig. S3A). This observation implies the potential for a functional association between miR-155-5p and TP53INP1 in fHP fibroblasts. Additionally, IHC of TP53INP1 revealed a substantial decrease of this protein in HP lung tissue compared to IPF. Interestingly, we found that TP53INP1 was overexpressed in areas of interstitial cells forming fibroblastic foci in IPF tissue but not in similar areas in tissue from patients with fHP. No specific signal was observed when the specific antibody was absent (Fig. S3B).

3.8. miR-155-5p expression promotes increased proliferation and decreased migration in normal human lung fibroblasts

To assess the potential impact of miR-155-5p on biological processes in normal human lung fibroblasts, we utilized an adenoviral system for gain-and-loss of function assays to regulate the miR-155-5p expression. Fig. 6A shows the transduction efficiency to increase (ON) or decrease (OFF) the expression of miR-155-p. Consequently, we examined the effects of miR-155-5p on TP53INP1 expression, proliferation, migration, and senescence markers in transduced normal human lung fibroblasts. Our results showed that higher expression of miR-155-5p causes a significant decrease in TP53INP1. Conversely, miR-155-5p inhibition leads to an increase in TP53INP1 expression (Fig. 6B). Next, we evaluated the effect of the miR-155-5p expression on the proliferation rate. Compared to control conditions, miR-155-ON significantly enhances the ability of

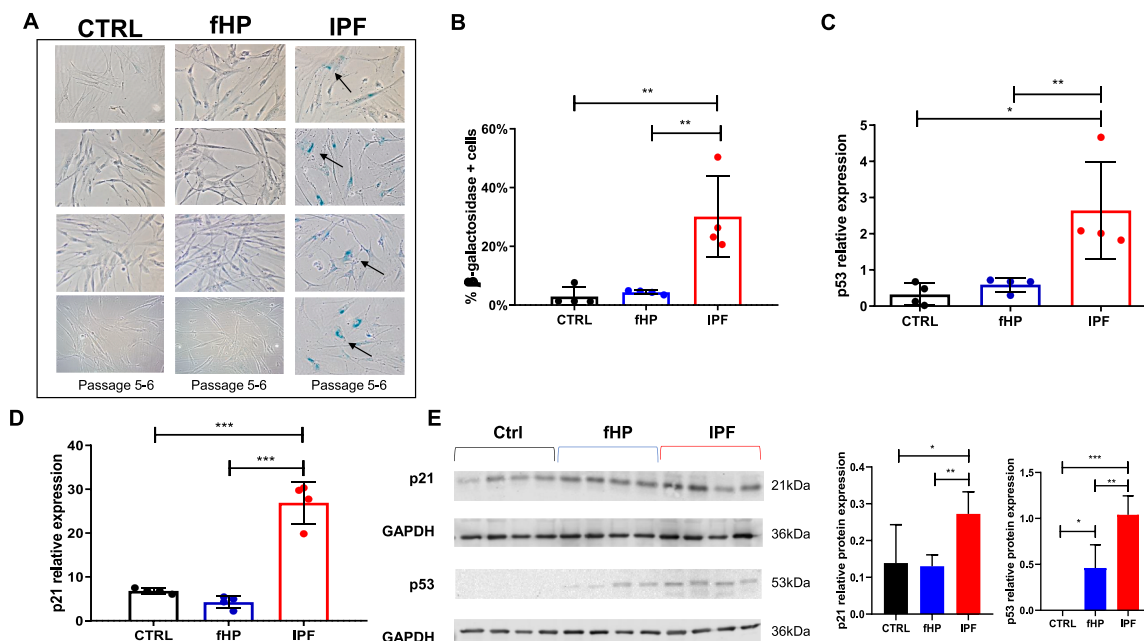


Fig. 3. fHP lung fibroblasts do not express senescence markers. (A) Representative images of β -galactosidase activity of fibroblasts at basal conditions ($n = 4$ per group). Black arrows point to positive staining (blue). (B) Graph of β -galactosidase positive cells ($n = 4$ per group). (C) qPCR relative expression of p53 (C) and p21 (D) in lung fibroblasts ($n = 4$ per group); (E) Blot of p53 and p21 in lung fibroblasts and graph of densitometric analysis of p21 and p53 relative to GAPDH ($n = 4$ per group). The bands of interest were cut from the original blots to create the image. Data are represented as the mean \pm SD. The P-value was calculated by one-way ANOVA. * $p < 0.05$; ** $p < 0.01$; *** $p < 0.001$.

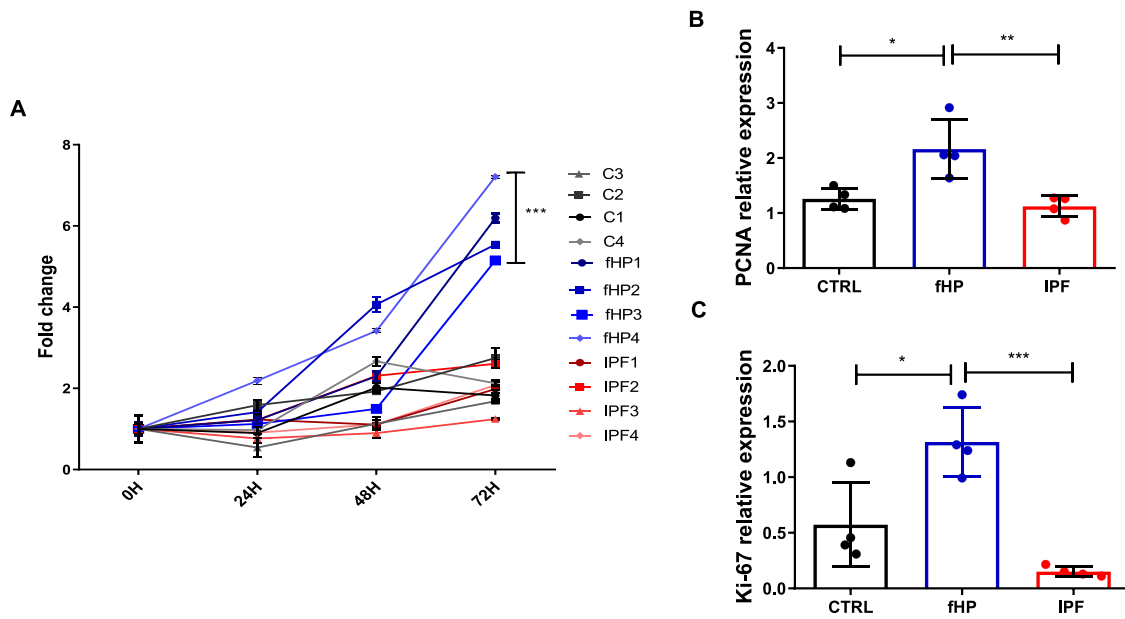


Fig. 4. Proliferation is increased in fHP lung fibroblasts. (A) Fibroblast proliferation was detected with CyQuant at 72h (n = 4 per group). qPCR relative expression of PCNA (B) and Ki-67 (C) in fibroblasts normalized to HPRT values. Data are represented as the mean ± SD of three independent experiments. ***p < 0.001 by two-way ANOVA.

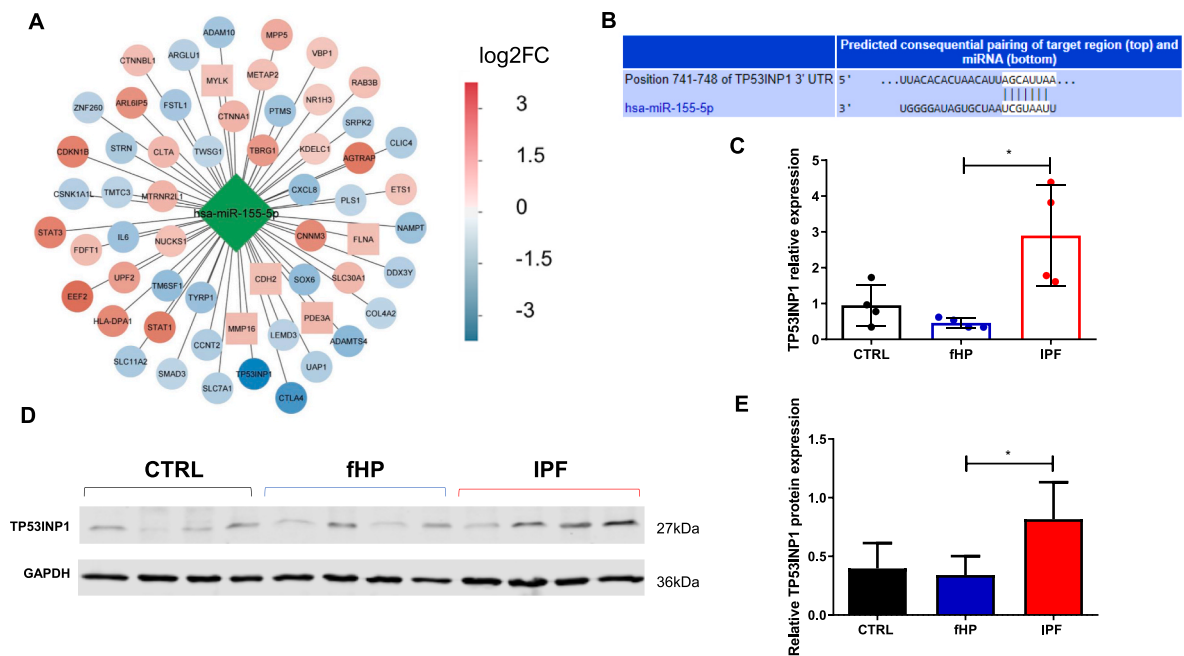


Fig. 5. TP53INP1 expression is decreased in fHP lung fibroblasts. (A) Regulatory interaction network generated in Cytoscape for DEGs between HP lungs and IPF lungs; red indicates that gene expression is upregulated; blue indicates that gene expression is downregulated in HP lungs compared to IPF lungs. Expression value was retrieved from GSE21369 (rectangles) and GSE150910 (circles). (B) Schematic representation shows the conserved miR-155 binding site of TP53INP1 3'-UTR. Retrieved from TargetScan database version 7.0 (<http://www.targetscan.org/>). (C) qPCR analysis of TP53INP1 in lung fibroblasts (n = 4 per group). Data were normalized to HPRT expression. (D) Blot of TP53INP1 in lung fibroblasts (n = 4 per group). The bands of interest were cut from the original blots to create the image. (E) Densitometric analysis of TP53INP1 immunoblots relative to GAPDH values * p < 0.05 by one-way ANOVA.

lung fibroblasts to proliferate. Meanwhile, miR-155-5p inhibition (miR-155 OFF) produced the opposite effects (Fig. 6C).

These outcomes are supported by the observation that augmenting miR-155-5p expression elevated the PCNA levels, and his loss decreased the expression of PCNA (Fig. 6D). Furthermore, the effect of miR-155-5p expression on migration was assessed through transwell experiments

(Fig. 6E). In this sense, overexpression of miR155-5p decreases the ability of fibroblasts to migrate, but its inhibition has no effect. A wound-healing assay supported these results (Fig. S4 A). Furthermore, we investigated the impact of miR-155-5p overexpression on senescence markers. Our results show that the loss of miR155-5p induced by transduction (OFF) causes a significant increase in the activity of

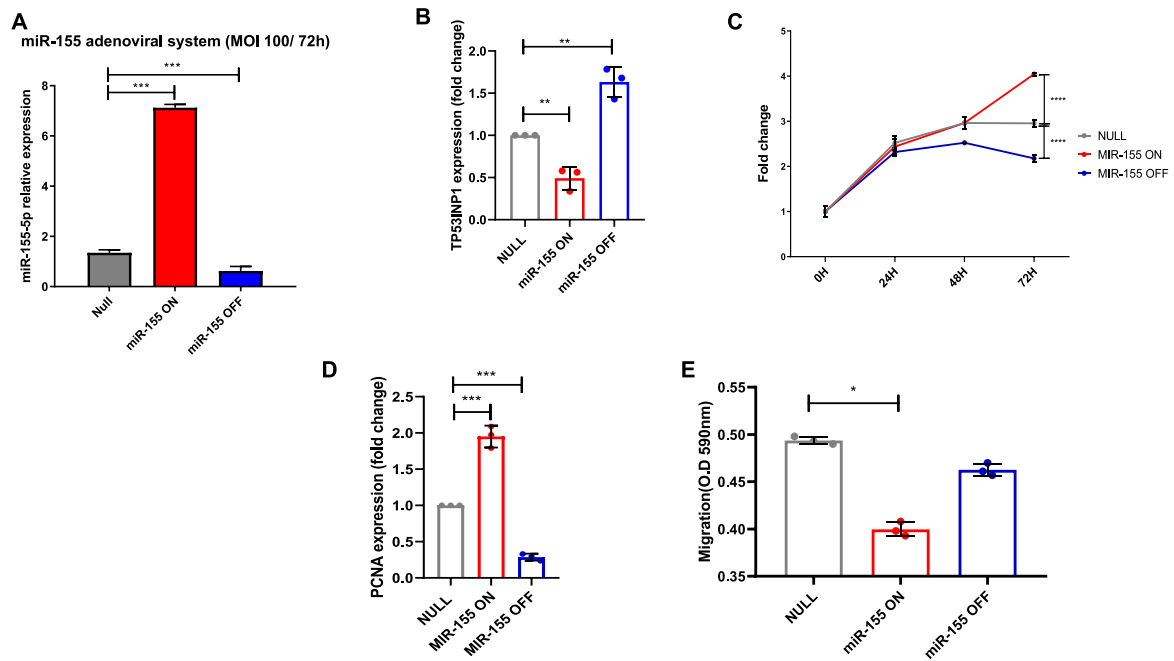


Fig. 6. miR-155-5p expression promotes increased proliferation and decreased migration in lung fibroblasts. Normal human lung fibroblasts were transduced with adenoviral particles of miR-155-5p-ON, miR-155-5p-OFF, or Null construction. (A) qPCR analysis of miR-155-5p after 72 h with adenoviral particles (MOI 100). (B) TP53INP1 expression measured by qPCR. Data was normalized to HPRT values. (C) Fibroblast proliferation was determined with CyQuant. (D) qPCR analysis of PCNA in transduced lung fibroblasts. (E) Migration measure by transwell invasion assay. The bars represent values of crystal violet staining at 590 nm. Data are represented as the mean ± SD. The P-value was calculated by one-way ANOVA *p < 0.05; **p < 0.01; ***p < 0.001.

β-galactosidase and the markers p21 and p53 (Fig. S4 B-D).

Additionally, lung fibroblasts are recognized as the leading producers of extracellular matrix. In this context, the inhibition of miR-155-5p significantly increases the production of fibrillar collagens COL1A1 and COL3A1 (Fig. S4 E). Our findings indicate that miR-155-5p can

modulate fibroblast phenotype by regulating proliferation, migration, senescence, and extracellular matrix collagen production.

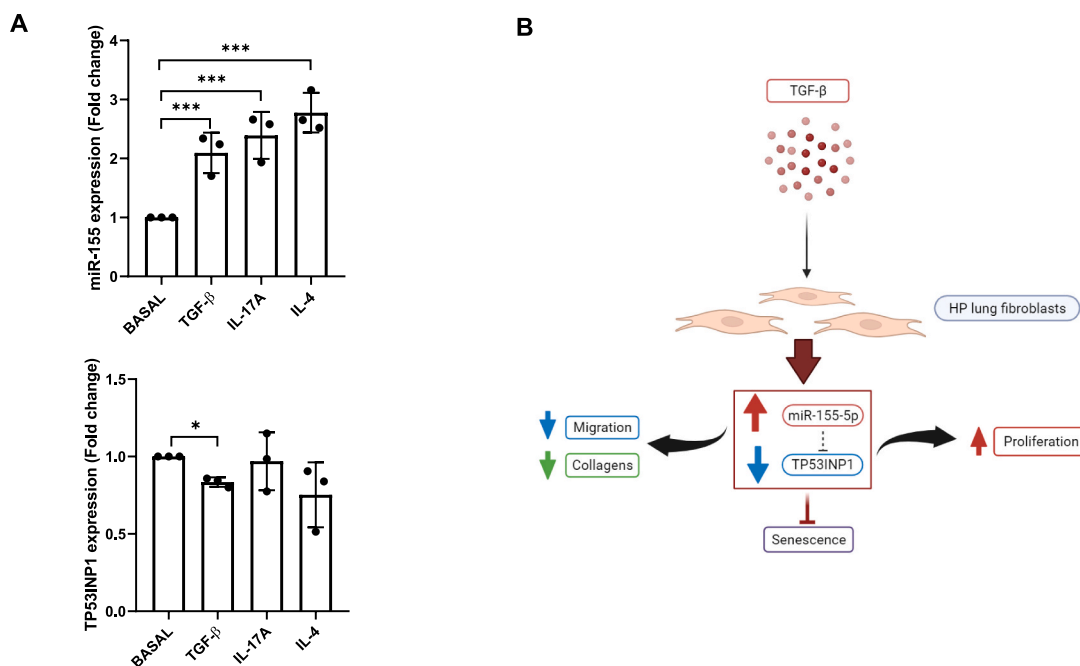


Fig. 7. TGF-β, IL-17A, and IL-4 induce miR-155-5p expression in lung fibroblasts. Analysis of miR-155-5p (A) and TP53INP1 (B) expression levels by qPCR following stimulation with TGF-β, IL-17A, and IL-4 at 10 ng/ml for 24h. *p < 0.05, ***p = 0.001. (C) A schematic representation shows the interaction among cytokines in the HP lung environment, miR-155-5p expression, TP53INP1 expression, and phenotypic features in fHP lung fibroblasts. Created with BioRender.com.

3.9. TGF- β , IL-17A, and IL-4 induce miR-155-5p expression in HP lung fibroblasts

Finally, as TGF- β , IL-17A, and IL-4 are cytokines associated with lung fibrosis [36,37], we evaluated their impact on miR-155-5p expression in HP lung fibroblasts *in vitro*. As shown in Fig. 7A, the treatment of fibroblasts with TGF- β , IL-17A, and IL-4 significantly enhanced the basal expression of miR-155-5p (Fig. 7A). However, only TGF- β stimulation provokes the opposite effect on TP53INP1 expression (Fig. 7B).

4. Discussion

In this study, we analyzed bulk RNA-seq data from HP lungs to identify a transcriptional signature and potential DEGs, and we found around 50 DEGs shared by several databases that differentiate HP from control and IPF lungs. Importantly, using mirTarBase, we identified 18 miRNAs that could regulate DEGs in HP lung, including miR-155-5p.

Gene enrichment analysis revealed several signaling pathways related to inflammatory response [19,20] and interferon response in HP. Interestingly, we found that CLDN18 is overexpressed in HP lungs compared to IPF lungs. This claudin is a lung-specific tight junction protein, the most abundant one in alveolar epithelial type I cells (AT1). Its deficiency in mice leads to impaired alveolarization and dysfunction of the alveolar epithelial barrier [38,39]. In sharp contrast, as suggested in our analysis, recent evidence by Gao et al. demonstrated that CLDN18 decreases in IPF compared with normal lungs, supporting the notion of the epithelial dysregulation that characterized this disease [40].

We also identified PLA2G2D over-expression in HP lungs relative to IPF lungs. PLA2G2D belongs to the phospholipase A2 family that may be involved in inflammation and immune response [41]. In this regard, lung fibroblasts of the PLA2G2A^{high} subpopulation are enriched in patients with fibrotic HP, which display greater angiogenesis activity and signatures of an inflammatory response, suggesting a role in pathogenesis [42].

Our study identified 18 potential key miRNAs implicated in HP pathogenesis. Notably, some of them (e.g., hsa-miR-92a-3p, hsa-miR-17-5p, and hsa-miR-20a/b) belong to the miR-17-92 cluster, which is epigenetically silenced in IPF lung fibroblasts [43]. However, our interest focused on the increased miR-155-5p, a multifunctional miRNA implicated in several cellular processes involved in the pathogenesis and progression of fibrosis, including proliferation and senescence [15,17]. Although the ontogenetic analysis did not show a significant upregulation of these pathways, which is not surprising since published omics data for HP are scarce and might be insufficient to enrich them, we decided to evaluate the possible impact of this miRNA since there is no related experimental data in isolated fibroblasts which are the primary cells orchestrating the fibrosing damage characteristic of these diseases. Additionally, proliferation and senescence are fundamental processes related to other pathways such as EMT, myogenesis, interferon response, or inflammatory response that we found to be increased in HP.

IPF is an irreversible, chronic, and fatal interstitial lung disease of unknown origin, primarily affecting older adults [44]. IPF is an age-related disease in which senescence in epithelial cells [45] and fibroblasts [46,47] has been reported, increasing the fibrotic response. In this sense, p53 is critical in regulating the increased cellular senescence in IPF fibroblasts [48]. Furthermore, it acts as a negative regulator of miR-155-5p [34]. Therefore, we investigated the expression of senescence markers, including p53, in lung fibroblasts. Surprisingly, we discovered that fHP fibroblasts, under basal conditions, do not exhibit senescence markers, such as p53, p21, and SA- β -galactosidase activity, unlike IPF fibroblasts, where the occurrence of these senescence markers is elevated [49].

MiR-155-5p is overexpressed in cancer and is essential to sustain cell proliferation [13]. Therefore, we analyzed the proliferation rate of HP lung fibroblasts and found that it increases cell division. Then, we analyzed the expression TP53INP1, a validated target of miR-155-5p

associated with proliferation. TP53INP1 belongs to a gene family containing two members, TP53INP1 and TP53INP2. The functions of TP53INP1 are involved in p53 activation and participate in cell survival and cycle arrest [50]. Our findings reveal a decrease of TP53INP1 in fHP fibroblasts compared to IPF fibroblasts and correlated with their high proliferation. Interestingly, this reduction was also observed in lung tissue from fHP patients, particularly in mesenchymal cell foci. These findings indicate that senescence is not a distinctive aspect of the typical fHP lung fibroblasts. By contrast, the proliferative phenotype of these cells may be a distinguishing hallmark, along with the upregulation of miR-155-5p, which may help differentiate them from other interstitial disorders, such as IPF.

Going deeper, we examined the role of miR-155-5p on two fundamental mechanisms in the biological function of lung fibroblasts: proliferation and migration by manipulating the miR-155-5p expression through an adenoviral system. Our results showed that miR-155-5p over-expression markedly increased the proliferation rate and the expression of proliferation markers, as well as reduced migratory capacity. The opposite results were obtained with miR-155-5p inhibition, which, in addition, caused an increase in some senescence markers, such as SA- β -galactosidase activity, p53, and p21 expression. These effects could be partially regulated by TP53INP1 expression, which was decreased when lung fibroblasts overexpressed miR-155-5p.

Finally, we investigated the impact of crucial cytokines, including TGF- β , IL-17A, and IL-4, on miR-155-5p and TP53INP1 expression; notably, all three cytokines induced miR-155-5p expression in fHP lung fibroblasts. A previous report found that this cytokine down-regulated miR-155-5p expression in normal fibroblasts [16]. However, the experiments were performed in only one commercially obtained line of fibroblasts. The abundance of cytokines in the HP lung environment may partially explain the heightened expression of miR-155-5p in fHP fibroblasts compared to IPF and control fibroblasts. However, only TGF- β provoked an increase in the expression of miR-155-5p and, concomitantly, a reduction of TP53INP1. Further studies are required to precise the role of TGF- β , IL-17A, and IL-4/miR-155-5p/TP53INP1 axis in HP lung fibroblasts.

It is important to emphasize that the function of miR-155-5p in different forms of pulmonary fibrosis is still controversial due to inconsistent findings in experimental models. For example, in one study, it was found that mice that lacked miR-155-5p^{-/-} demonstrated an enhanced fibrotic response caused by bleomycin [51]. Likewise, the use of antagomiR-155 mitigated alveolitis [52] and reduced histological changes and hydroxyproline levels in bleomycin or silicosis-induced pulmonary fibrosis models [53], indicating a putative profibrotic role of 155-5p.

However, other studies suggest that miR-155-5p may decrease the profibrotic phenotype induced by TGF- β [54,55], and moreover, another study reported that mice miR-155^{-/-} show lower fibrosis after bleomycin-induced lung injury than in wild-type mice [33], implying that it may have an anti-fibrotic role in pulmonary fibrosis. Further studies are required to determine the circumstances in which miR-155-5p exhibits anti- or profibrotic effects in lung fibrosis.

In summary, by integrating all existing bulk RNA-seq datasets, our study reveals the transcriptomic signature and associated miRNAs in HP lungs. Our collective findings show that the overexpression of miR-155-5p in fHP fibroblasts contributes to the high proliferative capacity of these cells due, in part, to a TP53INP1-dependent mechanism. Likely, the specific inflammatory microenvironment that surrounds these cells, which is characterized by the presence of cytokines such as TGF- β , IL-4, and IL-17, may, in part, be responsible for the proliferative phenotype which can distinguish them from other fibrotic conditions such as IPF (Fig. 7C). The candidate genes, pathways, and miRNAs identified in this study provide a foundation for future research in a field that is still poorly explored. The findings could improve the comprehension of the molecular and cellular mechanisms underlying HP and facilitate the identification of new therapeutic targets for this condition.

5. Conclusions

In conclusion, a transcriptional signature of 53 genes that may be useful to distinguish HP from IPF was identified. CLDN18, EEF2, CXCL9, PLA2G2D, and ZNF683 are potential targets for future studies. Additionally, 18 microRNAs may be helpful to establish differences between these two pathologies. Our results suggest that the balance between miR-155-5p and its target TP53INP1 is an essential part of the molecules that may influence the fibroblast phenotype characteristic of these fibrosing diseases; in particular, the overexpression of miR-155-5p in fHP and the decrease of TP53INP1 may be the cause of the increased proliferative profile in these cells. Our findings may help to differentiate and characterize their phenotype and to increase knowledge on this disease.

Funding

This research received no external funding.

Institutional review board statement

The study was conducted according to the guidelines of the Declaration of Helsinki and approved by the Bioethics Committee of Instituto Nacional de Enfermedades Respiratorias Ismael Cosío Villegas B09-13.

Informed consent statement

Informed consent was obtained from all subjects involved in the study, and their personal and identification data were protected.

Data availability statement

All the data are included in the manuscript.

Supplementary tables

Table S1: Primer sequences; Table S2: HP vs IPF; Table S3: GSE21369; Table S4: GSE150910; Table S5: common DEGs; Table S6: GSE21394; Table S7: common enrichment KEGG; Table S8: common enrichment GOBP; Table S9: miRNAs enrichment; Table S10: common miRNAs.

https://drive.google.com/drive/folders/1ooqD4S0h62_jjSSbRQiA_OuDVVntbYPU?usp=share_link

Additional files

R source code for running all the analysis documents in this manuscript is available at <https://github.com/canoscream/Non-coding-RNA-Research>.

CRedit authorship contribution statement

Marco Espina-Ordoñez: Writing – original draft, Visualization, Validation, Methodology, Investigation, Data curation. **Yalbi Itzel Balderas-Martínez:** Writing – review & editing, Visualization, Supervision, Software, Resources, Methodology, Data curation, Conceptualization. **Ana Lilia Torres-Machorro:** Supervision, Investigation. **Iliana Herrera:** Methodology. **Mariel Maldonado:** Methodology. **Yair Romero:** Methodology. **Fernanda Toscano-Marquez:** Methodology, Investigation. **Annie Pardo:** Writing – review & editing. **Moisés Selman:** Writing – review & editing. **José Cisneros:** Writing – review & editing, Supervision, Resources, Project administration, Conceptualization.

Declaration of competing interest

The authors declare no conflict of interest.

Acknowledgments

This paper serves as a fulfillment of Marco Antonio Espina-Ordoñez for obtaining a Ph.D. degree "Doctor en Ciencias", Campo de Conocimiento Biomedicina in the Posgrado en Ciencias Biológicas, UNAM and received the fellowship 717810 from Consejo Nacional de Ciencia y Tecnología (CONACYT), México. We also acknowledge the technical support of Miguel Ángel Pérez León of the Laboratorio de Cómputo de Alto Rendimiento, Coordinación del Departamento de Matemáticas, Facultad de Ciencias, UNAM. We thank LaNSBioDyT (CONACYT) for the technical support. The Fig. 7C and S1 were Created with BioRender.com.

Appendix A. Supplementary data

Supplementary data to this article can be found online at <https://doi.org/10.1016/j.ncrna.2024.02.010>.

References

- [1] F. Varone, B. Iovene, G. Sgalla, M. Calvella, A. Calabrese, A.R. Larici, L. Richeldi, Fibrotic hypersensitivity pneumonitis: diagnosis and management, *Lung* (2020), <https://doi.org/10.1007/s00408-020-00360-3>.
- [2] G. Raghu, B. Rochwerf, Y. Zhang, C.A. Garcia, A. Azuma, J. Behr, J.L. Brozek, H. R. Collard, W. Cunningham, S. Homma, T. Johkoh, An official ATS/ERS/JRS/ALAT clinical practice guideline: treatment of idiopathic pulmonary fibrosis. An update of the 2011 clinical practice guideline, *Am. J. Respir. Crit. Care Med.* (2015), <https://doi.org/10.1164/rccm.202005-2032ST>.
- [3] T. Okamoto, Y. Miyazaki, T. Ogura, K. Chida, N. Kohno, S. Kohno, H. Taniguchi, S. Akagawa, Y. Mochizuki, K. Yamauchi, H. Takahashi, A nationwide epidemiological survey of chronic hypersensitivity pneumonitis in Japan, *Respiratory investigation* (2013), <https://doi.org/10.1016/j.resinv.2013.03.004>.
- [4] N. Inase, Hypersensitivity pneumonitis: acute, chronic non-fibrotic, and chronic fibrotic, *Respiratory Investigation* (2021), <https://doi.org/10.1016/j.resinv.2021.09.005>.
- [5] H. Barnes, L. Troy, C.T. Lee, A. Sperling, M. Strek, I. Glaspole, Hypersensitivity pneumonitis: current concepts in pathogenesis, diagnosis, and treatment, *Allergy* (2022), <https://doi.org/10.1111/all.15017>.
- [6] T. Takemura, T. Akashi, H. Kamiya, S. Ikushima, T. Ando, M. Oritsu, M. Sawahata, T. Ogura, Pathological differentiation of chronic hypersensitivity pneumonitis from idiopathic pulmonary fibrosis/usual interstitial pneumonia, *Histopathology* (2012), <https://doi.org/10.1111/j.1365-2559.2012.04322.x>.
- [7] S.D. Alipoor, I.M. Adcock, J. Garssen, E. Mortaz, M. Varahram, M. Mirsaedi, A. Velayati, The roles of miRNAs as potential biomarkers in lung diseases, *Eur. J. Pharmacol.* (2016), <https://doi.org/10.1016/j.ejphar.2016.09.015>.
- [8] R.C. Friedman, K.K. Farh, C.B. Burge, D.P. Bartel, Most mammalian mRNAs are conserved targets of microRNAs, *Genome Res.* (2009), <https://doi.org/10.1101/gr.082701.108>.
- [9] S. O'Reilly, MicroRNAs in fibrosis: opportunities and challenges, *Arthritis Res. Ther.* (2016), <https://doi.org/10.1186/s13075-016-0929-x>.
- [10] H. Li, X. Zhao, H. Shan, H. Liang, MicroRNAs in idiopathic pulmonary fibrosis: involvement in pathogenesis and potential use in diagnosis and therapeutics, *Acta Pharm. Sin. B* (2016), <https://doi.org/10.1016/j.apsb.2016.06.010>.
- [11] D. Gulei, L. Raduly, E. Broseghini, M. Ferracin, I. Berindan-Neagoe, The extensive role of miR-155 in malignant and non-malignant diseases, *Mol. Aspect. Med.* (2019), <https://doi.org/10.1016/j.mam.2019.09.004>.
- [12] R. Mashima, Physiological roles of miR-155, *Immunology* (2015), <https://doi.org/10.1111/imm.12468>.
- [13] G. Higgs, F. Slack, The multiple roles of microRNA-155 in oncogenesis, *J. Clin. Bioinf.* (2013), <https://doi.org/10.1186/2043-9113-3-17>.
- [14] L. Ren, Y. Zhao, X. Huo, X. Wu, MiR-155-5p promotes fibroblast cell proliferation and inhibits FOXO signaling pathway in vulvar lichen sclerosis by targeting FOXO3 and CDKN1B, *Gene* (2018), <https://doi.org/10.1016/j.gene.2018.01.049>.
- [15] M.G. Eissa, C.M. Artlett, The microRNA miR-155 is essential in fibrosis, *Non-coding RNA* (2019), <https://doi.org/10.3390/ncrna5010023>.
- [16] N. Pottier, T. Maurin, B. Chevalier, M.P. Puisségur, K. Lebrigand, K. Robbe-Sermesant, T. Bertero, C.L. Lino Cardenas, E. Courcot, G. Rios, S. Fourre, Identification of keratinocyte growth factor as a target of microRNA-155 in lung fibroblasts: implication in epithelial-mesenchymal interactions, *PLoS One* (2009), <https://doi.org/10.1371/journal.pone.0006718>.
- [17] S. Zheng, Y. Zhang, Y. Hou, H. Li, J. He, H. Zhao, X. Sun, Y. Liu, Underlying molecular mechanism and construction of a miRNA-gene network in idiopathic pulmonary fibrosis by bioinformatics, *Int. J. Mol. Sci.* 24 (17) (2023 Aug 27) 13305, <https://doi.org/10.3390/ijms241713305>.
- [18] J.H. Cho, R. Gelinias, K. Wang, A. Etheridge, M.G. Piper, K. Batte, D. Dakhllallah, J. Price, D. Bornman, S. Zhang, C. Marsh, Systems biology of interstitial lung

- diseases: integration of mRNA and microRNA expression changes, *BMC Med. Genom.* (2011), <https://doi.org/10.1186/1755-8794-4-8>.
- [19] H. Furusawa, J.H. Cardwell, T. Okamoto, A.D. Walts, I.R. Konigsberg, J.S. Kurche, T.J. Bang, M.I. Schwarz, K.K. Brown, J.A. Kropski, M. Rojas, Chronic hypersensitivity pneumonitis, an interstitial lung disease with distinct molecular signatures, *Am. J. Respir. Crit. Care Med.* (2020), <https://doi.org/10.1164/rccm.202001-0134OC>.
- [20] M. Selman, A. Pardo, L. Barrera, A. Estrada, S.R. Watson, K. Wilson, N. Aziz, N. Kaminski, A. Zlotnik, Gene expression profiles distinguish idiopathic pulmonary fibrosis from hypersensitivity pneumonitis, *Am. J. Respir. Crit. Care Med.* (2006), <https://doi.org/10.1164/rccm.200504-6440C>.
- [21] J.L. Sepulveda, Using R and Bioconductor in clinical genomics and transcriptomics, *J. Mol. Diagn.* (2020), <https://doi.org/10.1016/j.jmoldx.2019.08.006>.
- [22] M.E. Ritchie, B. Phipson, D.I. Wu, Y. Hu, C.W. Law, W. Shi, G.K. Smyth, Limma powers differential expression analyses for RNA-sequencing and microarray studies, *Nucleic Acids Res.* (2015), <https://doi.org/10.1093/nar/gkv007>.
- [23] M.I. Love, W. Huber, S. Anders, Moderated estimation of fold change and dispersion for RNA-seq data with DESeq2, *Genome Biol.* (2014), <https://doi.org/10.1186/s13059-014-0550-8>.
- [24] M.V. Kuleshov, M.R. Jones, A.D. Rouillard, N.F. Fernandez, Q. Duan, Z. Wang, S. Koplev, S.L. Jenkins, K.M. Jagodnik, A. Lachmann, M.G. McDermott, C. D. Monteiro, G.W. Gundersen, A. Ma'ayan, Enrichr: a comprehensive gene set enrichment analysis web server 2016 update, *Nucleic Acids Res.* (2016), <https://doi.org/10.1093/nar/gkw377>.
- [25] A. Liberzon, C. Birger, H. Thorvaldsdóttir, M. Ghandi, J.P. Mesirov, P. Tamayo, The molecular signatures database hallmark gene set collection, *Cell systems* (2015), <https://doi.org/10.1016/j.cels.2015.12.004>.
- [26] H. Wickham, *ggplot2: Elegant Graphics for Data Analysis*, Springer-Verlag, New York, 2016. ISBN 978-3-319-24277-4. <https://ggplot2.tidyverse.org>.
- [27] V. Licursi, F. Conte, G. Fisco, P. Paci, MIENTURNET: an interactive web tool for microRNA-target enrichment and network-based analysis, *BMC Bioinf.* (2019), <https://doi.org/10.1186/s12859-019-3105-x>.
- [28] H.Y. Huang, Y.C. Lin, S. Cui, Y. Huang, Y. Tang, J. Xu, J. Bao, Y. Li, J. Wen, H. Zuo, W. Wang, J. Li, J. Ni, Y. Ruan, L. Li, Y. Chen, Y. Xie, Z. Zhu, X. Cai, X. Chen, L. Yao, Y. Chen, Y. Luo, S. LuXu, M. Luo, C.M. Chiu, K. Ma, L. Zhu, G.J. Cheng, C. Bai, Y. C. Chiang, L. Wang, F. Wei, T.Y. Lee, H.D. Huang, miRTarBase update 2022: an informative resource for experimentally validated miRNA-target interactions, *Nucleic Acids Res.* (2022), <https://doi.org/10.1093/nar/gkab1079>.
- [29] P. Shannon, A. Markiel, O. Ozier, N.S. Baliga, J.T. Wang, D. Ramage, N. Amin, B. Schwikowski, T. Ideker, Cytoscape: a software environment for integrated models of biomolecular interaction networks, *Genome Res.* (2003), <https://doi.org/10.1101/gr.1239303>.
- [30] J. Schindelin, I. Arganda-Carreras, E. Frise, V. Kaynig, M. Longair, T. Pietzsch, S. Preibisch, C. Rueden, S. Saalfeld, B. Schmid, J.Y. Tinevez, D.J. White, V. Hartenstein, K. Eliceiri, P. Tomancak, A. Cardona, Fiji: an open-source platform for biological-image analysis, *Nat. Methods* (2012), <https://doi.org/10.1038/nmeth.2019>.
- [31] M.W. Pfaffl, A. Tichopad, C. Prgommet, T.P. Neuvians, Determination of stable housekeeping genes, differentially regulated target genes and sample integrity: BestKeeper–Excel-based tool using pair-wise correlations, *Biotechnol. Lett.* (2004), <https://doi.org/10.1023/b:bile.0000019559.84305.47>.
- [32] One-way/Two-way ANOVA followed by Tukey's multiple comparisons test was performed using GraphPad Prism version 8.0.1 for Windows 10, GraphPad Software, Boston, Massachusetts USA, www.graphpad.com.
- [33] R.B. Christmann, A. Wooten, P. Sampaio-Barros, C.L. Borges, C.R. Carvalho, R. A. Kairalla, C. Feghali-Bostwick, J. Ziemek, Y. Mei, S. Goummih, J. Tan, miR-155 in the progression of lung fibrosis in systemic sclerosis, *Arthritis Res. Ther.* (2016), <https://doi.org/10.1186/s13075-016-1054-6>.
- [34] Y. Wang, M.N. Scheiber, C. Neumann, G.A. Calin, D. Zhou, MicroRNA regulation of ionizing radiation-induced premature senescence, *Int. J. Radiat. Oncol. Biol. Phys.* (2011), <https://doi.org/10.1016/j.ijrobp.2010.09.048>.
- [35] Y. Wang, T. Feng, S. Duan, Y. Shi, S. Li, X. Zhang, L. Zhang, miR-155 promotes fibroblast-like synovioyte proliferation and inflammatory cytokine secretion in rheumatoid arthritis by targeting FOXO3a, *Exp. Ther. Med.* (2020), <https://doi.org/10.3892/etm.2019.8330>.
- [36] K. Andrews, M.C. Ghosh, A. Schwingshackl, G. Rapalo, C. Luellen, C.M. Waters, E. A. Fitzpatrick, Chronic hypersensitivity pneumonitis caused by *Saccharopolyspora rectivirgula* is not associated with a switch to a Th2 response, *Am. J. Physiol. Lung Cell Mol. Physiol.* (2016), <https://doi.org/10.1152/ajplung.00305.2015>.
- [37] L. Barrera, F. Mendoza, J. Zuñiga, A. Estrada, A.C. Zamora, E.I. Melendro, R. Ramírez, A. Pardo, M. Selman, Functional diversity of T-cell subpopulations in subacute and chronic hypersensitivity pneumonitis, *Am. J. Respir. Crit. Care Med.* (2008), <https://doi.org/10.1164/rccm.200701-0930C>.
- [38] M.J. LaFemina, K.M. Sutherland, T. Bentley, L.W. Gonzales, L. Allen, C.J. Chapin, D. Rokkam, K.A. Sweerus, L.G. Dobbs, P.L. Ballard, J.A. Frank, Claudin-18 deficiency results in alveolar barrier dysfunction and impaired alveologenesis in mice, *Am. J. Respir. Cell Mol. Biol.* (2014), <https://doi.org/10.1165/rccb.2013-0456OC>.
- [39] A. Pardo, M. Selman, Idiopathic pulmonary fibrosis: new insights in its pathogenesis, *Int. J. Biochem. Cell Biol.* (2002), [https://doi.org/10.1016/s1357-2725\(02\)00091-2](https://doi.org/10.1016/s1357-2725(02)00091-2).
- [40] L. Gao, P. Li, H. Tian, M. Wu, J. Yang, X. Xu, Screening of biomarkers involved in idiopathic pulmonary fibrosis and regulation of upstream miRNAs, *Am. J. Med. Sci.* (2022), <https://doi.org/10.1016/j.amjms.2021.06.027>.
- [41] N. Suzuki, J. Ishizaki, Y. Yokota, K.I. Higashino, T. Ono, M. Ikeda, N. Fujii, K. Kawamoto, K. Hanasaki, Structures, enzymatic properties, and expression of novel human and mouse secretory phospholipase A2s, *J. Biol. Chem.* (2000), <https://doi.org/10.1074/jbc.275.8.5785>.
- [42] J. Wang, L. Zhang, L. Luo, P. He, A. Xiong, M. Jiang, Y. Liu, S. Liu, Q. Ran, D. Wu, Y. Xiong, Characterizing cellular heterogeneity in fibrotic hypersensitivity pneumonitis by single-cell transcriptional analysis, *Cell Death Discovery* (2022), <https://doi.org/10.1038/s41420-022-00831-x>.
- [43] D. Dakhllallah, K. Batte, Y. Wang, C.Z. Cantemir-Stone, P. Yan, G. Nuovo, A. Mikhail, C.L. Hitchcock, V.P. Wright, S.P. Nana-Sinkam, M.G. Piper, Epigenetic regulation of miR-17~92 contributes to the pathogenesis of pulmonary fibrosis, *Am. J. Respir. Crit. Care Med.* (2013), <https://doi.org/10.1164/rccm.201205-0888OC>.
- [44] G. Raghu, S.Y. Chen, W.S. Yeh, B. Maroni, Q. Li, Y.C. Lee, H.R. Collard, Idiopathic pulmonary fibrosis in US Medicare beneficiaries aged 65 years and older: incidence, prevalence, and survival, 2001–11, *Lancet Respir. Med.* (2014), [https://doi.org/10.1016/S2213-2600\(14\)70101-8](https://doi.org/10.1016/S2213-2600(14)70101-8).
- [45] S. Minagawa, J. Araya, T. Numata, S. Nojiri, H. Hara, Y. Yumino, M. Kawaiishi, M. Odaka, T. Morikawa, S.L. Nishimura, K. Nakayama, Accelerated epithelial cell senescence in IPF and the inhibitory role of SIRT6 in TGF- β -induced senescence of human bronchial epithelial cells, *Am. J. Physiol. Lung Cell Mol. Physiol.* (2011), <https://doi.org/10.1152/ajplung.00097.2010>.
- [46] H. Yanai, A. Shteinberg, Z. Porat, A. Budovsky, A. Braiman, R. Zeische, V. E. Fraifeld, Cellular Senescence-like Features of Lung Fibroblasts Derived from Idiopathic Pulmonary Fibrosis Patients, *Aging, Albany, NY*, 2015, <https://doi.org/10.18632/aging.100807>.
- [47] M. Schuliga, D.V. Pechkovsky, J. Read, D.W. Waters, K.E. Blokland, A.T. Reid, C. M. Hogaboam, N. Khalil, J.K. Burgess, C.M. Prêle, S.E. Mutsaers, Mitochondrial dysfunction contributes to the senescent phenotype of IPF lung fibroblasts, *J. Cell Mol. Med.* (2018), <https://doi.org/10.1111/jcmm.13855>.
- [48] D. Álvarez, N. Cárdenes, J. Sellarés, M. Bueno, C. Corey, V.S. Hanumanthu, Y. Peng, H. D'Cunha, J. Sembrat, M. Nouraei, S. Shanker, IPF lung fibroblasts have a senescent phenotype, *Am. J. Physiol. Lung Cell Mol. Physiol.* (2017), <https://doi.org/10.1152/ajplung.00220.2017>.
- [49] M.J. Schafer, T.A. White, K. Iijima, A.J. Haak, G. Ligresti, E.J. Atkinson, A.L. Oberg, J. Birch, H. Salmonowicz, Y.I. Zhu, D.L. Mazula, Cellular senescence mediates fibrotic pulmonary disease, *Nat. Commun.* (2017), <https://doi.org/10.1038/ncomms14532>.
- [50] H. Saadi, M. Seillier, A. Carrier, The stress protein TP53INP1 plays a tumor suppressive role by regulating metabolic homeostasis, *Biochimie* (2015), <https://doi.org/10.1016/j.biochi.2015.07.024>.
- [51] M. Kurowska-Stolarska, M.K. Hasoo, D.J. Welsh, L. Stewart, D. McIntyre, B. E. Morton, S. Johnstone, A.M. Miller, D.L. Asquith, N.L. Millar, A.B. Millar, The role of microRNA-155/liver X receptor pathway in experimental and idiopathic pulmonary fibrosis, *J. Allergy Clin. Immunol.* (2017), <https://doi.org/10.1016/j.jaci.2016.09.021>.
- [52] X. Sun, Y. Kang, S. Xue, J. Zou, J. Xu, D. Tang, H. Qin, In vivo therapeutic success of MicroRNA-155 antagonist in a mouse model of pulmonary fibrosis induced by bleomycin, *Kor. J. Intern. Med.* (2021), <https://doi.org/10.3904/kjim.2019.098>.
- [53] Y. Chen, D. Xu, J. Yao, Z. Wei, S. Li, X. Gao, W. Cai, N. Mao, F. Jin, Y. Li, Y. Zhu, Inhibition of miR-155-5p exerts anti-fibrotic effects in silicotic mice by regulating meprin α , *Mol. Ther. Nucleic Acids* (2020) <https://doi.org/10.1016/j.omtn.2019.11.018>.
- [54] L. Chu, Y. Li, X. Zhang, X. Fu, Z. Zhu, MicroRNA-155 inhibits the pro-fibrogenic activities of TGF- β 1 in human lung fibroblasts, *Int. J. Clin. Exp. Med.* 10 (2017) 347–356.
- [55] L. Chi, Y. Xiao, L. Zhu, M. Zhang, B. Xu, H. Xia, Z. Jiang, W. Wu, microRNA-155 attenuates profibrotic effects of transforming growth factor-beta on human lung fibroblasts, *J. Biol. Regul. Homeost. Agents* (2019), <https://doi.org/10.23812/19-41A>.